www.sciencemag.org/content/360/6385/223/suppl/DC1

Supplementary Materials for

Germinal center antibody mutation trajectories are determined by rapid self/foreign discrimination

Deborah L. Burnett, David B. Langley, Peter Schofield, Jana R. Hermes, Tyani D. Chan, Jennifer Jackson, Katherine Bourne, Joanne H. Reed, Kate Patterson, Benjamin T. Porebski, Robert Brink, Daniel Christ,* Christopher C. Goodnow*

*Corresponding author. Email: d.christ@garvan.org.au (D.C.); c.goodnow@garvan.org.au (C.C.G.)

Published 13 April 2018, *Science* **360**, 223 (2018)
DOI: 10.1126/science.aao3859

This PDF file includes:

Other Supplementary Material for this manuscript includes the following:
(available at www.sciencemag.org/content/360/6385/223/suppl/DC1)

Materials and Methods

Mice

All mice used in the experiments were bred at Australian BioResources and held at the Garvan Institute of Medical Research in specific pathogen-free environments. The Garvan Animal Ethics Committee approved all mice protocols and procedures. C57BL/6 (non-transgenic) mice were purchased from the Australian BioResources (Moss Vale, New South Wales). HyHEL10-transgenic (SW_{HEL}) mice have been described previously (*10*). These mice carry a single copy V_H10 anti-HEL heavy chain variable region coding exon targeted to the endogenous Igh^b allele plus multiple copies V_H10-κ anti-HEL light chain transgene. SW_{HEL} mice on a CD45.1 congenic ($Ptprc^{a/a}$) C57BL/6 background were also homozygous $Rag1^{-/-}$, (*26)* which prevented endogenous Ig variable region gene rearrangements so that all B-cells expressed the HyHEL10 B-cell receptor (BCR).

HEL^{3X} is an R21Q, R73E, and D101R triply mutated HEL protein (*13*). HEL^{3X} binds to HyHEL10 with relatively low affinity of $K_a = 1.19 \times 110^7\ M^{-1}$ (*14*). Transgenic mice on the C57BL/6 background expressed HEL^{3X} as an integral cell surface protein, by addition at the C-terminus of the transmembrane segment and cytoplasmic tail of the $H2K^b$ class I major histocompatibility protein (*14*). The transgene was controlled by the human ubiquitin C (*UBC*) promoter, resulting in membrane bound HEL^{3X} expression on the surface of all nucleated and anucleate cells. HEL^{3X} membrane expression was confirmed using flow cytometric binding to HyHEL9 on RBC and WBC (*14*).

Bone marrow chimeras

Recipient mice of 8-12 weeks of age were lethally irradiated (2x425 cGy) using an X-RAD 320 Biological Irradiator (Precision X-Ray, North Branford, CT, UA). Femoral, humeral, and tibial bone marrow cells were aspirated into B-cell medium (BCM) comprising RPMI (Gibco, Carlsbad, CA, USA) with 10% heat-inactivated Fetal Calf Serum (FCS) (Gibco), 2 mM L-glutamine, 100 U/mL penicillin RPMI media (Gibco). Fifteen hours after irradiation recipient mice were transplanted with an intravenous injection of 5-10 × 10^6 bone marrow cells. For $mHEL^{3X}$ transgenic ($CD45.2^+$) recipients, injected bone marrow cells were 80% of $SW_{HEL}.Rag1^{-/-}$ ($CD45.1^+$) origin and 20% of $mHEL^{3X}$ transgenic ($CD45.2^+$) origin. As previously observed (*15*), $CD45.2^+$ pre-B-cells lacking pre-rearranged *Igh* and *Igk* genes proliferated more than their SW_{HEL} ($CD45.1^+$) Ig transgenic counterparts, so that only ~5% of $B220^+$ in chimeric recipients were $CD45.1^+$ anti-HEL B-cells. Initially (fig S3), chimeras produced in control non-transgenic C57BL/6 ($CD45.2^+$) mice also used a bone marrow cell mix that was 80% $SW_{HEL}.Rag1^{-/-}$ ($CD45.1^+$) and 20% recipient-matched (wild-type $CD45.2^+$). Subsequently, control non-transgenic mice were reconstituted with less (45%) $SW_{HEL}.Rag1^{-/-}$ ($CD45.1^+$) and more (55%) wild-type ($CD45.2^+$) bone marrow, so that comparable frequencies of anti-HEL B-cells in the transitional subset of the spleen were obtained in chimeras irrespective of self-antigen ($mHEL^{3X}$) expression. Chimeras were analyzed 8-14 weeks after reconstitution.

Immunohistology

Five-to-seven-micron sections were cut using a Leica CM1900 cryostat, fixed in acetone and blocked with 30% normal horse serum. To stain HyHEL10 B-cells, sections were incubated with 200 ng/mL HEL (Sigma, St Louis, MO, USA), polyclonal rabbit anti-HEL sera, and anti-rabbit-IgG-FITC (Rockland Immunochemicals, Pottstown, PA, USA). T-cells were stained with anti-CD3-biotin (eBiosciences, San Diego, CA, USA) and streptavidin-AlexaFlour 555 (Invitrogen, Carlsbad, CA, USA). Follicular B-cells were stained with anti-IgD- AlexaFlour 647 (Biolegend, San Diego, CA, USA). For GC analysis, GCs were stained with anti-CD16/CD32-PE (BD Pharmingen, San Diego, CA, USA) and CD3-biotin stains were followed by streptavidin-BV421 (BD Pharmingen). Stained tissue sections were imaged using a Zeiss Leica DM5500 microscope. AxioVision software was used for image capture and Adobe Photoshop used to compile the images. Images shown are 200X magnification.

In vitro cultures

B-cell responses in vitro were determined by culturing fresh splenocytes overnight at 37 °C in BCM following red-blood-cell lysis. B-cells were stimulated with one of the following additives: HEL^{WT} (200 ng/mL), LPS (2.5 μg/mL, Sigma), recombinant mouse IL-4 (10 ng/mL, R&D Systems, Minneapolis, MN) or anti-IgM mAb (5 μg/mL, Southern Biotech, Birmingham, AL, USA). Cells were then surface stained to detect the upregulation of CD86 by flow cytometry.

Alternatively, fresh splenocytes were resuspended at 2×10^7 cells/mL in PBS containing 5% FCS and CFSE labeled with a final concentration of 11 μM for 5 minutes at room temperature. Cells were washed in PBS containing 5% FCS and then resuspended in BCM. B-cells were stimulated with anti-CD40 mAb (5 μg/mL, BD Pharminigen), LPS, anti-IgM mAb, IL-4, HEL^{WT} plus LPS, anti-CD40 mAb plus IL-4, HEL^{WT} plus IL-4 or anti-IgM mAb plus IL-4. Cells were cultured for 3 days at 37 °C proliferation was assessed as loss of CFSE staining via flow cytometry.

Recombinant HEL proteins

Purified HEL^{WT} was purchased from Sigma-Aldrich. Recombinant HEL^{3X} and DEL proteins were made as secreted proteins in *Pichia pastoris* yeast (Invitrogen) and purified from culture supernatants by ion exchange chromatography as previously described (*10, 13, 14*). For the purposes of crystallography, DEL lacking a poly-histidine affinity tag was purified from duck eggs as described elsewhere *(27)*. Proteins were stored in PBS at 1-2.5 mg/mL at -80 °C. Prior to use samples were thawed and stored at 4°C for a maximum of 8 months.

Sheep red blood cell (SRBC) conjugation

HEL proteins were desalted into conjugation buffer (distilled water with 0.35 M D-Mannitol [Sigma] and 0.01 M Sodium Chloride [Sigma]). For this process PD-10 columns (Amersham, Piscataway, NJ, USA) were equilibrated with 30 mL Conjugation buffer. One hundred micrograms of protein was loaded onto each column and pushed through the column using 2.5 mL Conjugation buffer. For elution of the protein, 3.5 mL conjugation buffer was added and the HEL protein collected as fractions in the following volumes; 250 μL, 1000 μL, 250 μL, 250 μL, 250 μL. Protein concentrations of each

fraction were determined by spectrophotometry.

For conjugation, SRBC were washed in 30 mL of PBS per 6-8 × 10^9 cells. Washing was performed three times by centrifugation at 2,300 rpm (1,111 g) for 5 min at 4 °C in PBS and then once in conjugation buffer. SRBC were then resuspended in a final volume of 1 mL conjugation buffer in a 50 mL Falcon tube containing 10 μg/mL of protein for conjugation, unless otherwise stated, which had first been buffer exchanged by gel filtration on PD10 columns into the conjugation buffer. The solution was mixed on a platform rocker on ice for 10 minutes. One hundred microliters of 100 mg/mL N-(3-Dimethylaminopropyl)-N-ethylcarbodimide hydrochloride (Sigma) was then added and the solution was mixed for a further 30 minutes on ice. SRBCs were then washed four times in 30 mL PBS. Confirmation of successful conjugation was performed by flow-cytometric analysis of SRBC using AlexaFluor 647-conjugated HyHEL9 antibody. 2 × 10^8 conjugated or unconjugated SRBC were injected into the lateral tail vein of each chimeric mouse.

Flow cytometry

On the day of harvest organs were collected into BCM, cell suspensions passed through a 70 μm cell strainer (Falcon, Corning, NY, USA) and centrifuged 1 500 rpm (440 g) for 5 min at 4 °C. Fc receptors were blocked with unlabeled anti-CD16/32 (ebioscience) before staining. To detect HEL^{3X}-binding cells, cells were stained with 2 μg/mL (0.14 μM) HEL^{3X}, followed by AlexaFluor 647-conjugated HyHEL9. Since this concentration of HEL^{3X} approximates the K_a of the unmutated HyHEL10 receptor on the B-cells, it occupied approximately half of the binding sites(*14*).

For DEL-N terminal biotinylation, DEL was conjugated to 5 M excess of NHS biotin (Sigma) at pH 6.5 overnight on ice. For panels where DEL-biotin staining was concurrently used with HyHEL9, HyHEL9 stains were followed with HEL^{4X} at 2 μg/mL to block any unbound HyHEL9 binding sites without binding to the HyHEL10 BCR. DEL-biotin staining then followed at 2 μg/mL.

Anti-IgG_1 -FITC (BD Pharmingen) stains were followed by 5% mouse serum before staining for other surface molecules. Cells were filtered using 35 μm filter round-bottom FACS tubes (BD Pharmingen) immediately before data acquisition on a LSR II analyzer (BD Pharmingen).

Forward- and side-scatter threshold gates were applied to remove red blood cells and debris and approximately 5-7 × 10^6 events were collected per sample. Cytometer files were analyzed with FlowJo software (FlowJo LLC, Ashland, Oregon, USA).

BrdU staining

BrdU staining was performed as described previously (*16*). Briefly mice were given drinking water shielded from light containing 0.8 mg/mL BrdU (Sigma). Spleens and bone marrow were prepared as for flow cytometry. Following surface staining cells were fixed and permeabilized, DNA denatured and then stained with anti-BrdU FITC using BrdU staining kit (BD Phaminigen) as per the manufacturer's directions.

Fab expression and purification

Mutant and wild-type HyHEL10 heavy (*IgH*) and wild-type HyHEL10 kappa-light (*IgK*) chain FAb sequences were synthesized and cloned into pCEP4 expression vector via *Kpn*I and *Bam*HI restriction sites. The heavy chain was C-terminally his-tagged for purification purposes. Fab arms were transiently expressed using the Expi293 Expression System (Thermo Fisher Scientific, Boston, MA, USA) according to the manufacturer's recommendations. Lipid-DNA complexes were prepared using a 1H:2L chain ratio, as previously described *(28)*. Fab was purified from cell culture supernatant using HisTrap FF crude columns (GE Healthcare, Little Chalfont, UK) according to the manufacturer's instructions. After dialysis against PBS Fabs were concentrated using spin filters (EMD Millipore, Billerica, MA, USA), inspected on SDS-PAGE and their concentrations determined by spectrometry (absorbance at 280 nm).

Analysis of binding affinity

Purified HyHEL10 FAbs were buffer exchanged into PBS using equilibrated ZebaSpin columns (Thermo Fisher Scientific). FAb samples were requantified and incubated with EZ-Link NHS-PEG4-Biotinylation reagent (Thermo Fisher Scientific) at a 5:1 biotin-to-protein ratio. Free biotin was removed from the samples by repeating the buffer exchange step in a second zebaspin column equilibrated with PBS.

Affinity of interactions between biotinylated FAbs and purified lysozyme proteins (DEL and HEL^{3X}) by Biolayer Interferometry (BLItz, ForteBio, Menlo Park, CA, USA). Streptavidin biosensors were rehydrated in PBS containing 0.1% w/v BSA for 1 hr at RT. Biotinylated FAb was loaded onto the sensors "on-line" using an advanced kinetics protocol, and global fits were obtained for the binding kinetics by running associations and dissociations of Lysozyme proteins at a suitable range of molar concentrations. The global dissociation constant (KD) for each 1:1 FAb-lysozyme interaction was determined using the BlitzPro 1.2.1.3 software.

Single cell FACS sorting

Cell suspensions were prepared and germinal center B-cells identified as for flow cytometry. Single-cell sorting into 96-well plates (Thermo Fisher Scientific) was performed on a FACSAria or FACSAriaIII (BD Pharminigen). B-cells from each mouse were analyzed individually to ensure over-representation of one particular clone did not affect mutation analysis. The VDJ_H exon of the HyHEL10 heavy chain gene was amplified from genomic DNA by PCR, sequenced, and analyzed as previously described (*14*).

ELISA

ELISA detection of serum concentrations of IgG_1 antibodies binding to HEL^{3X}/DEL were measured as previously described (*10*). High-binding plates (Corning, Corning, NY, USA) were coated with HEL^{3X} or DEL and bound serum antibody quantified using the same IgH chain isotype-specific secondary antibodies used for flow cytometry. Antibody levels were quantified against HyHEL10 standards.

Crystallography

The complex comprising DEL purified from duck eggs (isoform DEL-I) and the Fab arm of HyHEL10^{I29F,S52T,Y53F} (HH10*3) was prepared by gel filtration chromatography in which a 2:1 ratio of DEL:HH10*3 was applied to an S200 26/60 column (GE Healthcare) plumbed with 25 mM Tris (pH 8.5), 150 mM NaCl. Crystals of HH10*3-DEL were grown by hanging drop vapor diffusion whereby 2 μL of protein complex (at ~6.5 mg/mL) was combined with an equal volume of well solution comprising 100 mM sodium citrate (pH 4.75 and 17 % v/v) PEG3350 (Hampton Research, Aliso Viejo, CA, USA). Crystals grew over several weeks. Crystals were briefly swum (10 sec) in well solution doped with glycerol to ~25 % (v/v) prior to being flash frozen in N_2 (l sec) for data collection.

Diffraction data, structure solution and refinement

Diffraction data were collected at the Australian Synchrotron on beamline MX2 at 100 K. Diffraction data were indexed and integrated using iMOSFLM (*29*), the space group determined with POINTLESS (*30*), and scaling performed with AIMLESS (*31*). Structures were solved via molecular replacement using PHASER (*32*) and employing PDB entries 3D9A (Fab) and 5V8G (DEL-I) (27) as search models. Rigid-body and restrained B-factor refinement were performed with REFMAC5 (*33*), part of the CCP4 suite of crystallography software. Models were inspected and compared with electron density maps, and where necessary modified, using COOT (*34*). Validation was performed using the MOLPROBITY server (*35*).

Quantification and statistical analysis

GraphPad Prism 6 (GraphPad Software, San Diego, USA) was used for data analysis. When the data were normally distributed, an unpaired Student's *t*-test was performed for analysis. When data was not normally distributed Welsh's correction was applied. For all tests, $P < 0.05$ was considered as being statistically significant. Unless otherwise stated error bars represent arithmetic mean. Flow cytometric plots of multiple samples are presented as mean and standard error or mean. For all figures, data points indicate individual mice. * represents $P < 0.05$, ** represents $P < 0.01$, *** represents $P < 0.001$, **** represents $P < 0.0001$.

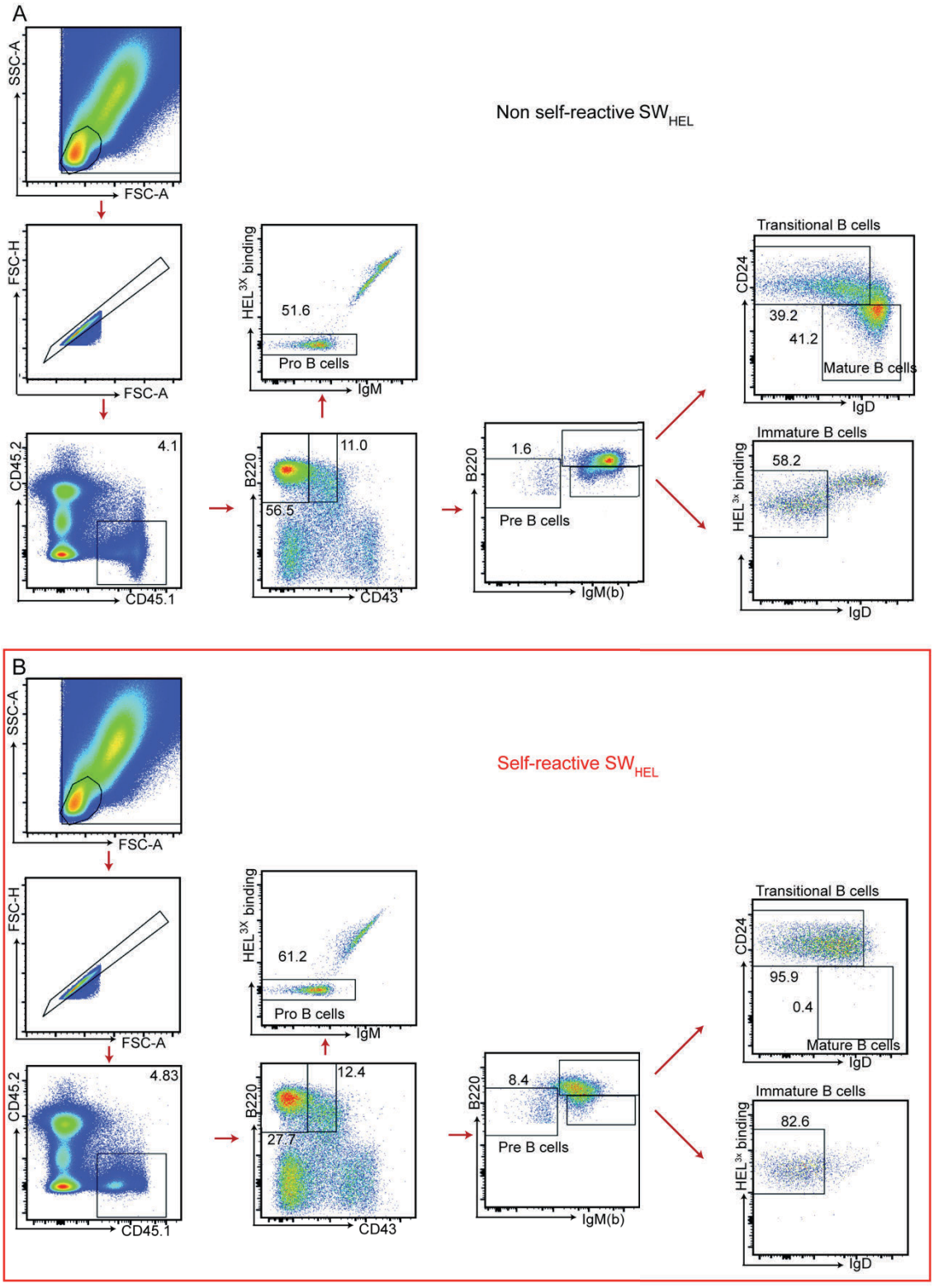

Fig. S1.
Gating strategy used to identify subsets of SW_{HEL} B-cells in the bone marrow.

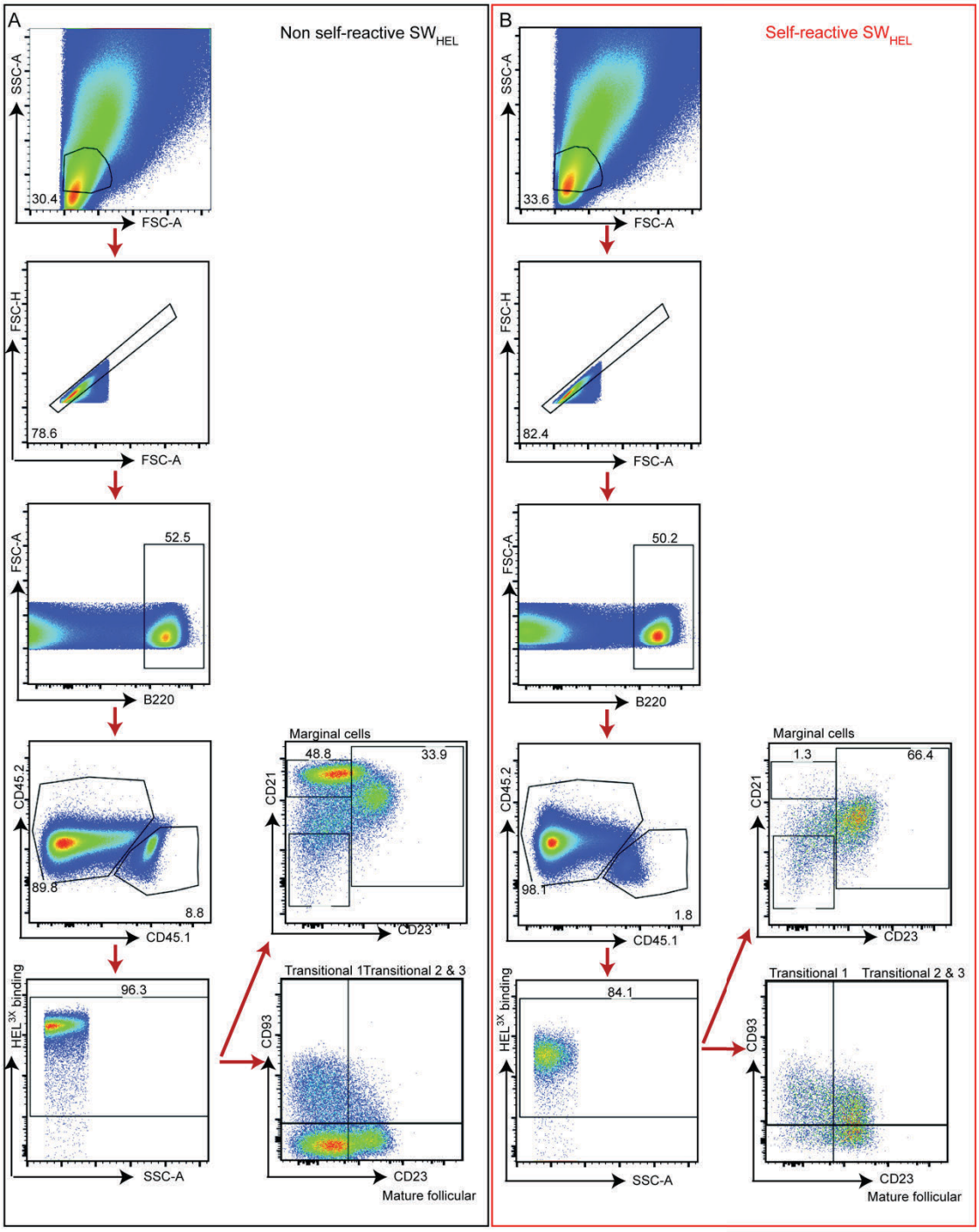

Fig. S2

Gating strategy used to identify subsets of SW_{HEL} B-cells in the spleen.

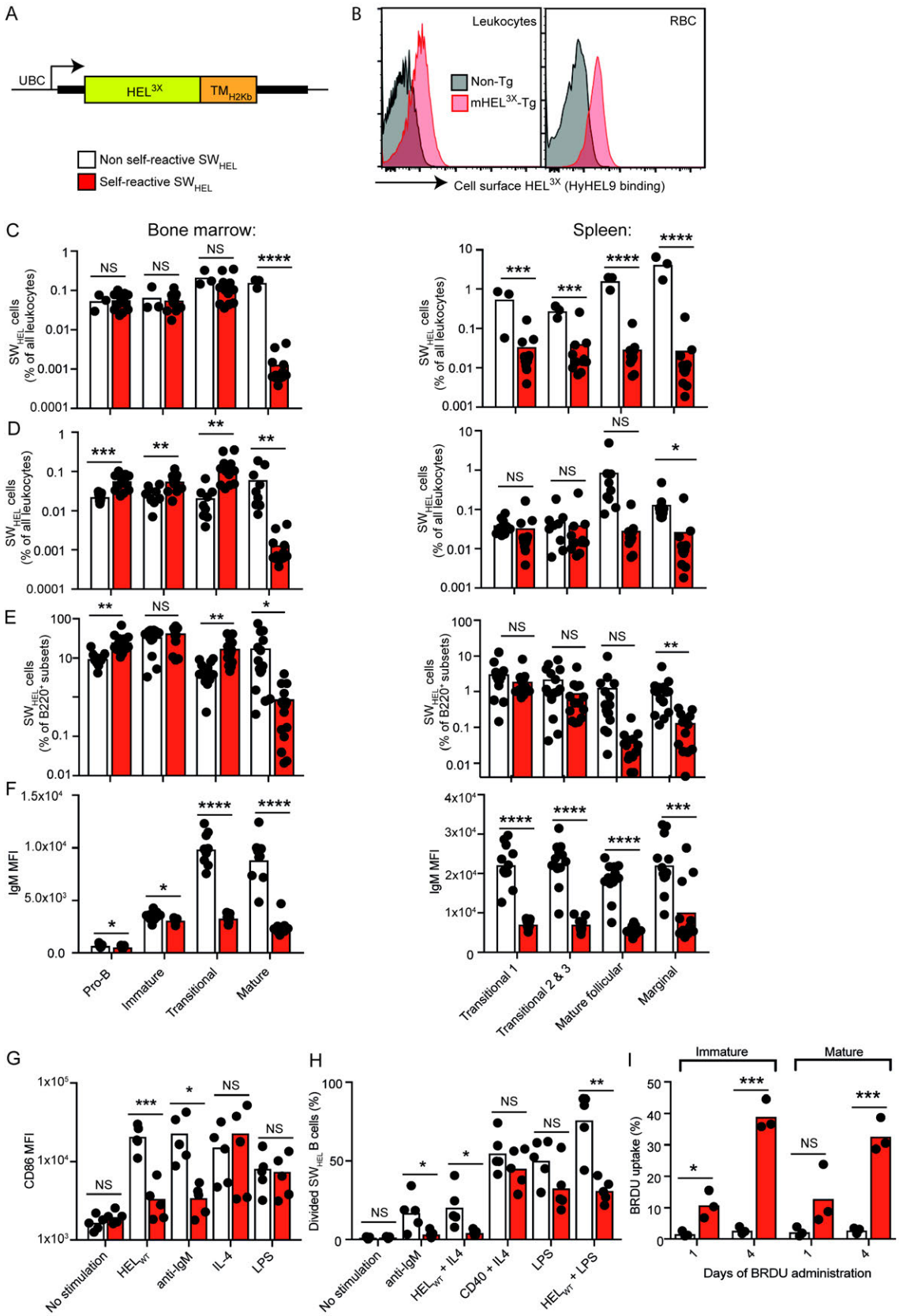
A
UBC
HEL3X
TMH2Kb
Non self-reactive SWHEL
Self-reactive SWHEL
B
Leukocytes
RBC
Non-Tg
mHEL3X-Tg
Cell surface HEL3X (HyHEL9 binding)
C
Bone marrow:
Spleen:
SWHEL cells (% of all leukocytes)
D
SWHEL cells (% of all leukocytes)
E
SWHEL cells (% of B220+ subsets)
F
IgM MFI
Pro-B
Immature
Transitional
Mature
Transitional 1
Transitional 2 & 3
Mature follicular
Marginal
G
CD86 MFI
No stimulation
HELWT
anti-IgM
IL-4
LPS
H
Divided SWHEL B cells (%)
No stimulation
anti-IgM
HELWT + IL4
CD40 + IL4
LPS
HELWT + LPS
I
Immature
Mature
BRDU uptake (%)
Days of BRDU administration

Fig. S3

Fig S3 (cont'd) SW_{HEL} B-cells become anergic in response to self-HEL^{3X} displayed at low density on the surface of other hematopoietic and non-hematopoietic cells.
(**A**) Schematic of the *UBC*:*mHEL*^{3X} transgene integrated at the *Rosa26* locus. (**B**) Staining for cell surface HEL^{3X} on leukocytes and RBC from transgenic ($mHEL^{3X}$-Tg) or wild-type non-transgenic (non-tg) B6 mice. (**C**) Frequency of the indicated subsets of SW_{HEL} B-cells among all leukocytes in the bone marrow and spleen of chimeric mice reconstituted with 80% SW_{HEL} *Rag1*$^{-/-}$ CD45.1 and 20% B6 non-tg or B6 $mHEL^{3X}$-tg bone marrow. Data points are for individual chimeras; n=3 non self-reactive SW_{HEL} and n= 11 for self-reactive $SW_{HEL.}$ (**D, E**) Frequency of the indicated subsets of SW_{HEL} B-cells among all leukocytes (D), or among that subset of total B220+ cells (E), in the bone marrow and spleen of chimeric mice reconstituted with 80% SW_{HEL} *Rag1* $^{-/-}$ CD45.1 and 20% $mHEL^{3X}$-tg marrow (self-reactive SW_{HEL}; n≥11) or 45% SW_{HEL} *Rag1* $^{-/-}$ CD45.1 and 55% non-tg marrow (Non self-reactive SW_{HEL}; n≥9). (**F**) Cell surface IgM mean fluorescence intensity (MFI), in the bone marrow and spleen of chimeras as in (D). For bone marrow N= 9 per group. For spleen N= 12 for non self-reactive SW_{HEL} and N= 11 for self-reactive $SW_{HEL.}$ (**F, G**) CD86 induction (**F**) and proliferation (**G**), gated on $B220^{+}CD45.1^{+}HEL^{+}$ SW_{HEL} spleen cells from separate chimeras marrow transplanted as in (**D**) cultured with the indicated stimuli. N=5 per group. (**H**) Turnover of immature ($CD45.1^{+}HEL^{+}CD93^{+}$) or mature ($CD45.1^{+}HEL^{+}CD93^{-}$) SW_{HEL} B-cells in the spleen in chimeras described in (**D**) given BrdU in the drinking water for the indicated times. n= 3 per group.
Data points represent one mouse. NS P>0.05, * P<0.05, ** P<0.01, *** P<0.001, **** P<0.0001. Student's *t*-test. Data pooled from at least two independent experiments.

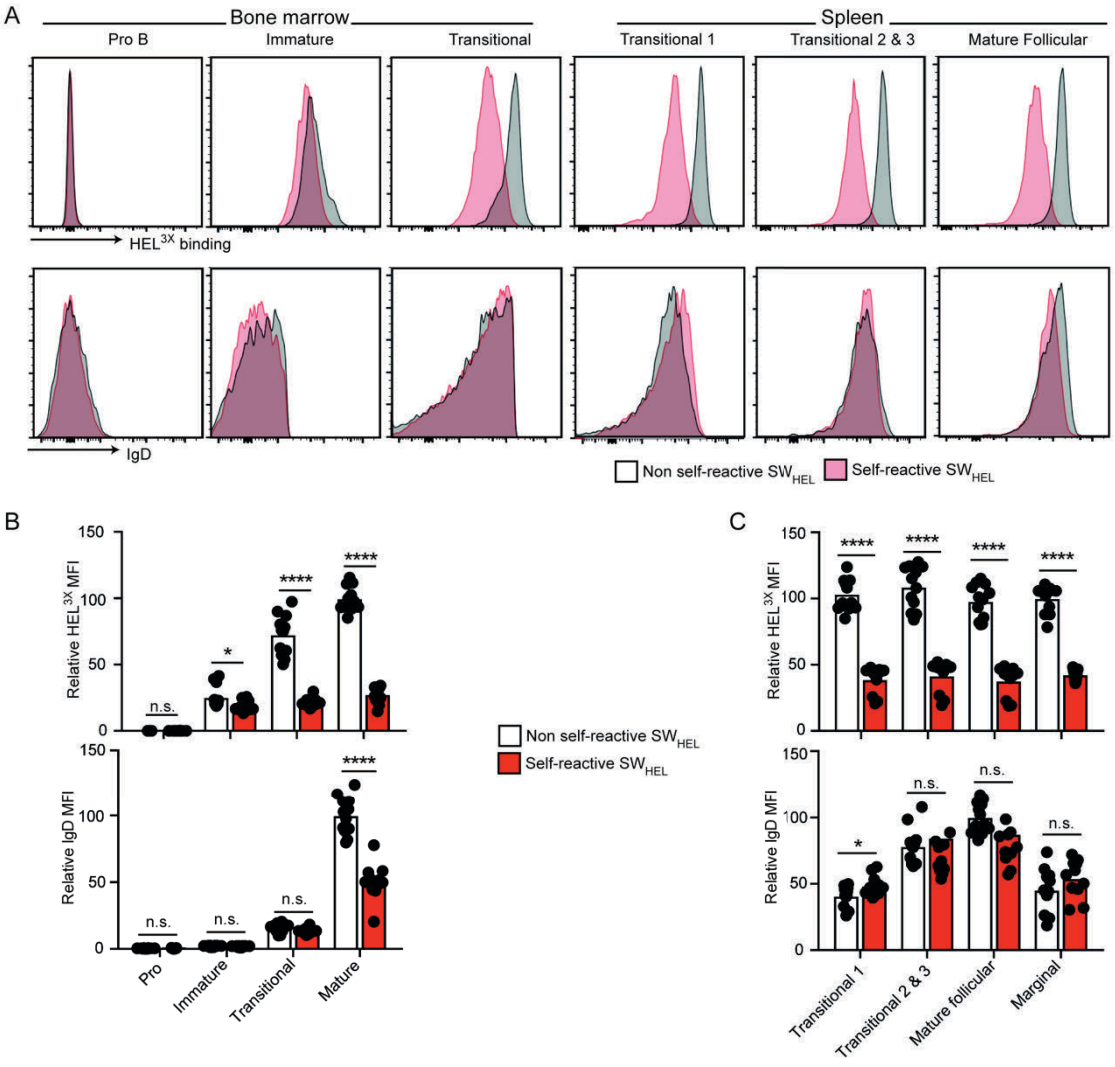

Fig. S4.

Expression of antigen receptors on the surface of SW_{HEL} B-cells at different stages of maturation.

(**A**) Representative surface histograms of HEL^{3X} (0.14 μM) binding and cell surface IgD and (**B, C**) mean fluorescent intensity (MFI) on the indicated subsets of SW_{HEL} B-cells in individual chimeric mice, relative to the mean of the mature non-self-reactive B-cells in all mice in the same experiment, and arithmetic means..

Data points represent one mouse. n=11-12 per group. Data pooled from two independent experiments. NS P>0.05, * P<0.05, ** P<0.01, **** P<0.0001. Student's *t*-test.

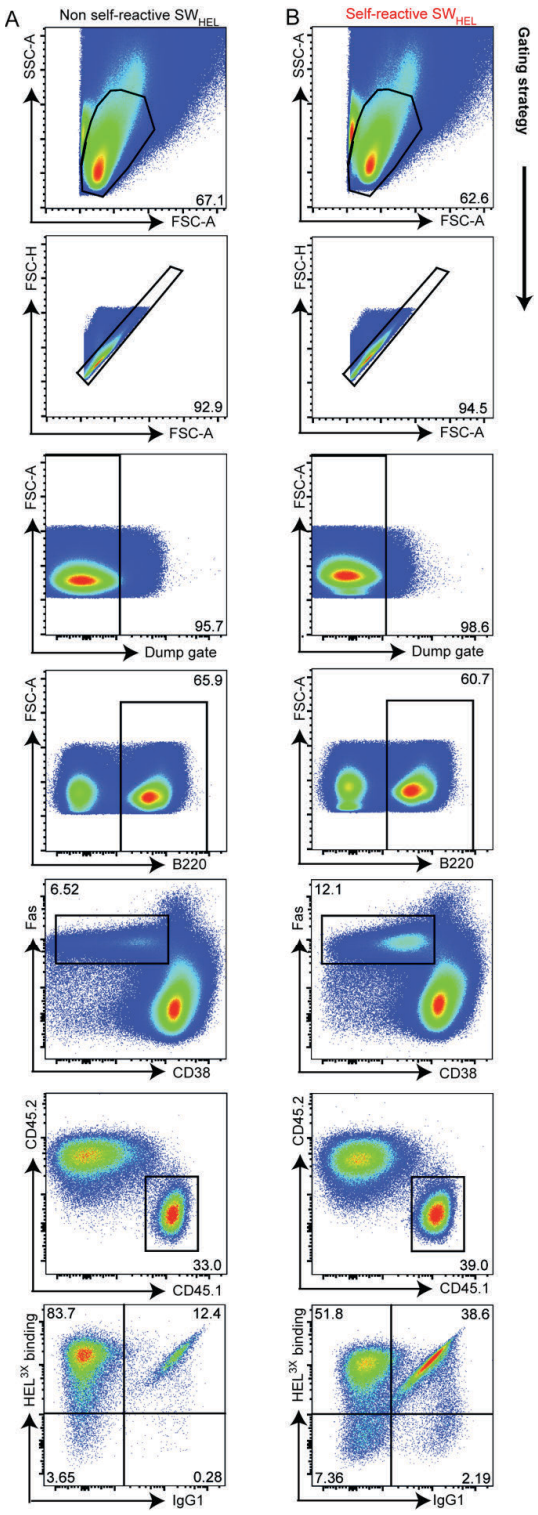

Fig. S5.

Representative flow cytometric profiles and gates applied to spleen cells from mice with non self-reactive (**A**) or self-reactive (**B**) SW_{HEL} B-cells, immunized with unconjugated SRBC on day 0 and with SRBC conjugated to 10 µg/mL DEL on day 11, with splenocytes analyzed on day 15.

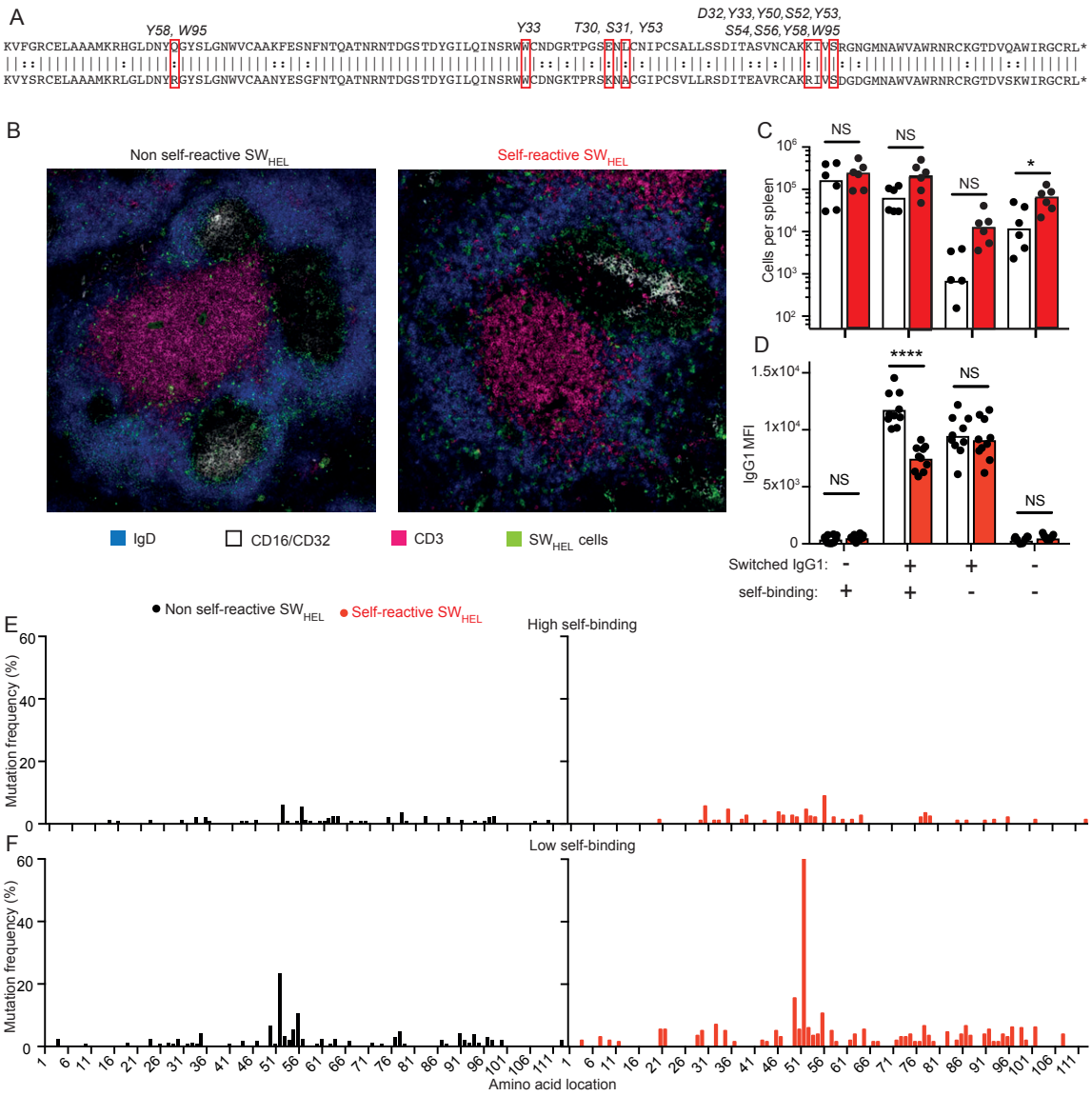

Fig. S6.

Effects of self- and foreign- antigen binding on SW$_{HEL}$ B-cells 4 days after recruitment into GC reactions.

Mice were first immunized with unconjugated SRBC to initiate GC reactions and boosted with DEL-SRBC 11 days after to activate SW$_{HEL}$ cells and their spleens analyzed 4 days following DEL-SRBC immunization. (**A**) Self (HEL^{3X}-top) and foreign (DEL-bottom) protein sequences. Boxed amino acids contact the amino acid heavy chain residues listed in italics. (**B**) Representative immnohistological microscopy of the spleen showing IgD (blue) marking follicular mantles around GCs, CD3 (magenta) marking the T-cell zone, CD16/CD32 (white) marking follicular dendritic cells in the GC light zone, and HEL binding cells in green. (**C**) Total numbers of the B220^{+}Fas^{+}CD38^{-}CD45.1^{+}CD45.2^{-} SW$_{HEL}$ GC B-cells per spleen from the quadrants outlined in figure 2. N=6 per group. (**D**) Cell surface IgG1 MFI of the B220^{+}Fas^{+}CD38^{-}CD45.1^{+}CD45.2^{-} SW$_{HEL}$ GC B-cells from the quadrants outlined in figure 2. n=10 per group. (**E,F**) SW$_{HEL}$ GC B-cells were

sorted using the quadrants shown in Figure 2 into cells with high or low binding to 0.14uM HEL^{3X}, regardless of switched status, and single cells sequenced. Graphs show % of cells with substitutions at each H-chain amino acid in single SW_{HEL} GC cells with high (**E**) or low (**F**) self-binding, in single cell sorted non self-reactive (black) and self-reactive (red) GC SW_{HEL} B-cells.

Data points represent one mouse. Data pooled from at least two independent experiments. NS P>0.05, * P<0.05, **** P<0.0001. Student's *t*-test.

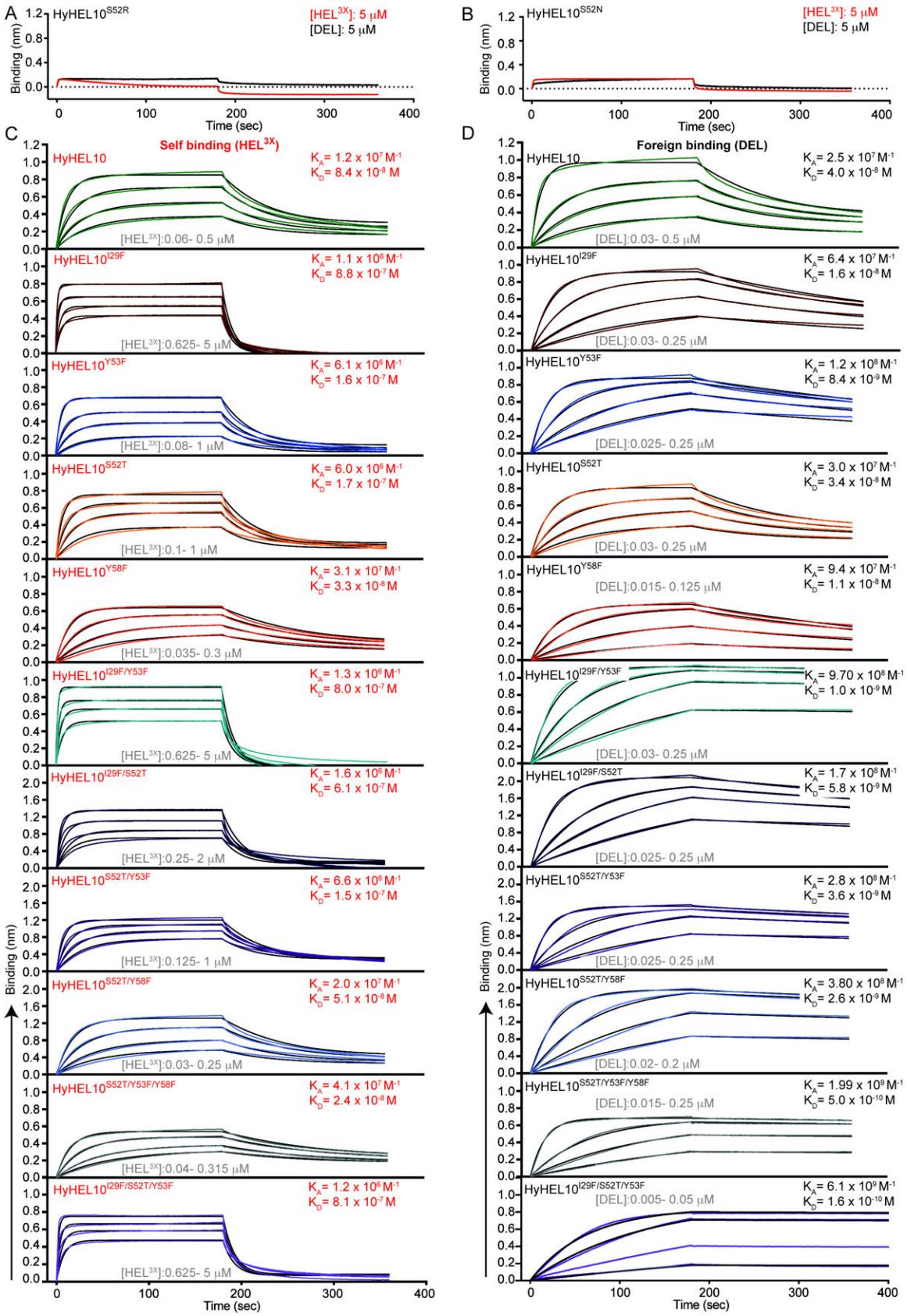
A
HyHEL10S52R
[HEL3X]: 5 μM
[DEL]: 5 μM
Binding (nm)
Time (sec)
B
HyHEL10S52N
[HEL3X]: 5 μM
[DEL]: 5 μM
C
Self binding (HEL3X)
HyHEL10
KA= 1.2 x 10^7 M-1
KD= 8.4 x 10-8 M
[HEL3X]:0.06- 0.5 μM
HyHEL10I29F
KA= 1.1 x 10^8 M-1
KD= 8.8 x 10-7 M
[HEL3X]:0.625- 5 μM
HyHEL10Y53F
KA= 6.1 x 10^6 M-1
KD= 1.6 x 10-7 M
[HEL3X]:0.08- 1 μM
HyHEL10S52T
KA= 6.0 x 10^6 M-1
KD= 1.7 x 10-7 M
[HEL3X]:0.1- 1 μM
HyHEL10Y58F
KA= 3.1 x 10^7 M-1
KD= 3.3 x 10-8 M
[HEL3X]:0.035- 0.3 μM
HyHEL10I29F/Y53F
KA= 1.3 x 10^8 M-1
KD= 8.0 x 10-7 M
[HEL3X]:0.625- 5 μM
HyHEL10I29F/S52T
KA= 1.6 x 10^6 M-1
KD= 6.1 x 10-7 M
[HEL3X]:0.25- 2 μM
HyHEL10S52T/Y53F
KA= 6.6 x 10^6 M-1
KD= 1.5 x 10-7 M
[HEL3X]:0.125- 1 μM
HyHEL10S52T/Y58F
KA= 2.0 x 10^7 M-1
KD= 5.1 x 10-8 M
[HEL3X]:0.03- 0.25 μM
HyHEL10S52T/Y53F/Y58F
KA= 4.1 x 10^7 M-1
KD= 2.4 x 10-8 M
[HEL3X]:0.04- 0.315 μM
HyHEL10I29F/S52T/Y53F
KA= 1.2 x 10^6 M-1
KD= 8.1 x 10-7 M
[HEL3X]:0.625- 5 μM
D
Foreign binding (DEL)
HyHEL10
KA= 2.5 x 10^7 M-1
KD= 4.0 x 10-8 M
[DEL]:0.03- 0.5 μM
HyHEL10I29F
KA= 6.4 x 10^7 M-1
KD= 1.6 x 10-8 M
[DEL]:0.03- 0.25 μM
HyHEL10Y53F
KA= 1.2 x 10^8 M-1
KD= 8.4 x 10-9 M
[DEL]:0.025- 0.25 μM
HyHEL10S52T
KA= 3.0 x 10^7 M-1
KD= 3.4 x 10-8 M
[DEL]:0.03- 0.25 μM
HyHEL10Y58F
KA= 9.4 x 10^7 M-1
KD= 1.1 x 10-8 M
[DEL]:0.015- 0.125 μM
HyHEL10I29F/Y53F
KA= 9.70 x 10^8 M-1
KD= 1.0 x 10-9 M
[DEL]:0.03- 0.25 μM
HyHEL10I29F/S52T
KA= 1.7 x 10^8 M-1
KD= 5.8 x 10-9 M
[DEL]:0.025- 0.25 μM
HyHEL10S52T/Y53F
KA= 2.8 x 10^8 M-1
KD= 3.6 x 10-9 M
[DEL]:0.025- 0.25 μM
HyHEL10S52T/Y58F
KA= 3.80 x 10^8 M-1
KD= 2.6 x 10-9 M
[DEL]:0.02- 0.2 μM
HyHEL10S52T/Y53F/Y58F
KA= 1.99 x 10^9 M-1
KD= 5.0 x 10-10 M
[DEL]:0.015- 0.25 μM
HyHEL10I29F/S52T/Y53F
KA= 6.1 x 10^8 M-1
KD= 1.6 x 10-10 M
[DEL]:0.005- 0.05 μM

Fig. S7.

(Fig. S7 cont'd) Association and dissociation of soluble monomeric self (HEL^{3X}) or foreign (DEL) protein binding to biotinylated HyHEL10 antibody Fab mutants immobilized onto streptavidin biosensors, as measured by bio-layer interferometry. (**A,B**) No detectable binding of soluble self (red) or foreign (black) antigen to immobilized (**A**) $HyHEL10^{S52R}$ or (**B**) $HyHEL10^{S52N}$ at a concentration of 5 μM. (**C,D**) Association and dissociation of monomeric self (**C**) or foreign (**D**) antigen binding to immobilized HyHEL10 mutant variants. Soluble antigen was run over immobilized HyHEL10 Fab at four different concentrations to obtain global fits of binding kinetics for each interaction using the BLItz Pro 1.2 software (ForteBio). The utilized concentrations of antigen differed for each HyHEL10 variant, but all fell within a range between 5 nM (lowest foreign molarity used for $HyHEL10^{I29F/S52T/Y53F}$) to 5 μM (highest self molarity used for $HyHEL10^{I29F}$, $HyHEL10^{I29F/Y53F}$ and $HyHEL10^{I29F/S52T/Y53F}$). Affinity binding constants (K_A, M^{-1}) and equilibrium dissociation constants (K_D, M) are also shown for each interaction.

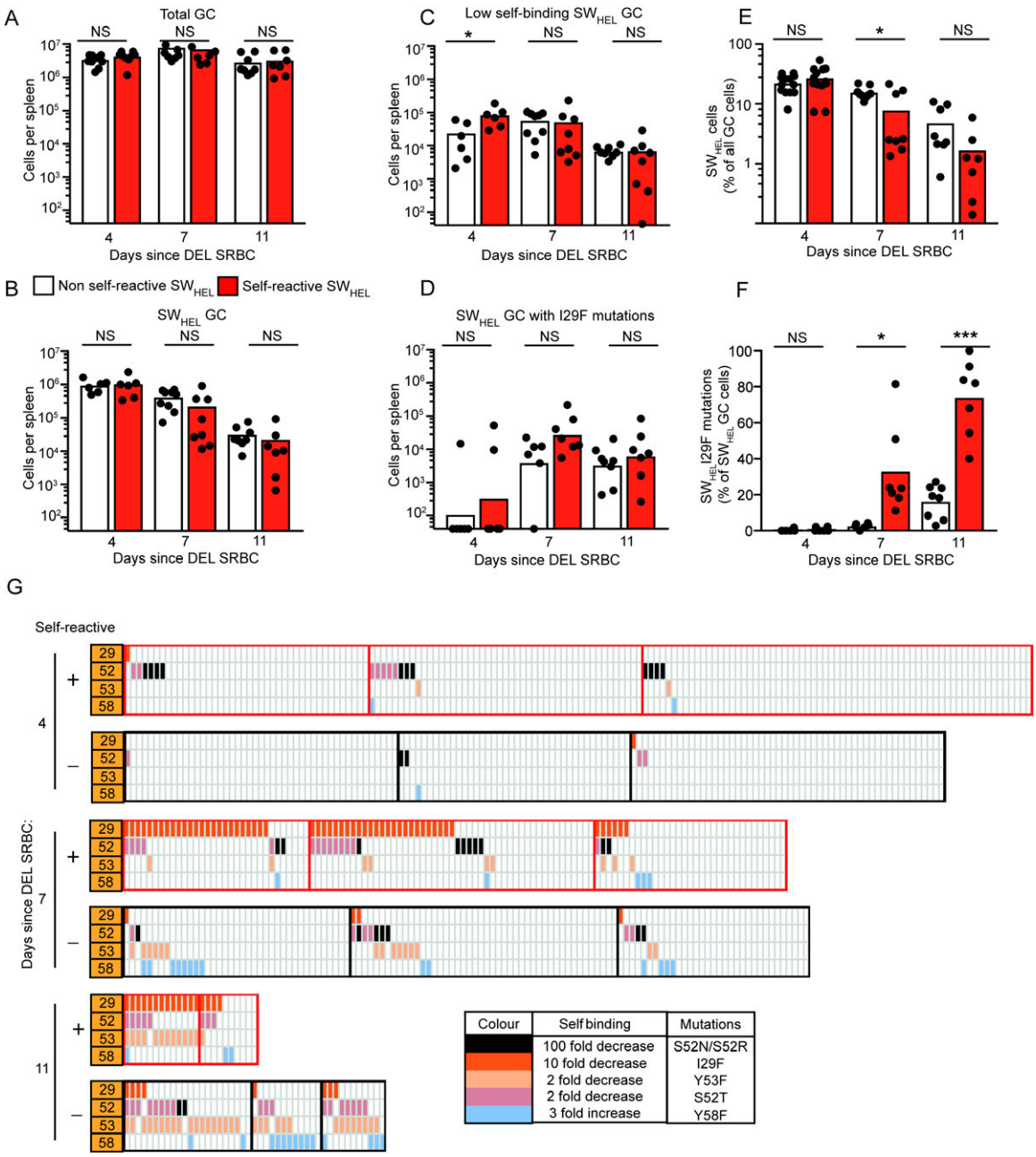

Fig. S8.

Details of SW_{HEL} cell frequencies and mutations for individual mice and individual cells for the experiment shown in Figure 3A. Mice were first immunized with unconjugated SRBC to initiate GC reactions and boosted with DEL-SRBC to activate SW_{HEL} cells and their spleens analyzed 4, 7 and 11 days following DEL-SRBC immunization as shown in figure 3A. (**A**) Total GC cells ($B220^{+}Fas^{+}CD38^{-}$) per spleen from individual mice at the indicated timepoints. (**B**) Total SW_{HEL} GC ($B220^{+}Fas^{+}CD38^{-}CD45.1^{+}CD45.2^{-}$) per spleen from individual mice at the indicated timepoints. (**C**) Total SW_{HEL} GC per spleen that do not bind to HEL^{3X} at 0.14μM from individual mice at the indicated timepoints. (**D**) Total SW_{HEL} GC per spleen bearing I29F mutations from individual mice at the indicated timepoints. (**E**) The percentage of $CD45.1^{+}$ SW_{HEL} cells among total GC cells

at the indicated timepoints. (**F**) The percentage of CD45.1$^+$ SW_{HEL} cells bearing I29F mutations at the indicated timepoints. (**G**) Summary of mutations at H-chain I29, S52, Y53, and Y58 in individual sorted SW_{HEL} cells. Color coding denotes the consequence of each mutation for self-affinity. Each column represents a single cell, each row denotes whether that cell has a mutation at the indicated amino acid position, and all the cells from a single mouse are grouped within red or black boxes.
Data points represent one mouse. NS $P>0.05$, * $P<0.05$. Student's *t*-test. Data in A-F pooled from two independent experiments. Data in G are from one experiment, representative of two, each involving 2-3 mice per timepoint.

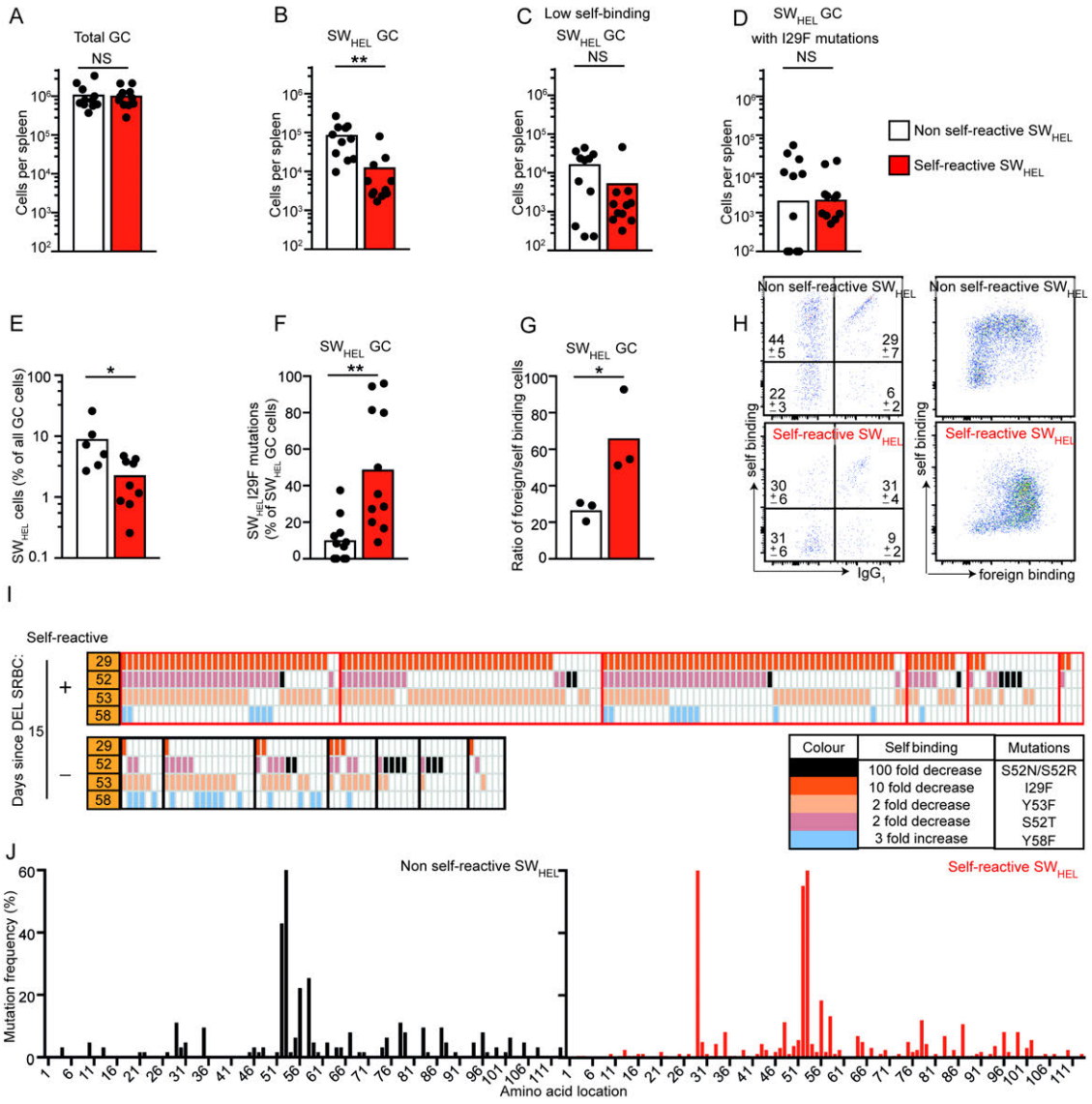

Fig. S9.

Details of SW_{HEL} cell frequencies and mutations for individual mice and individual cells for the experiment shown in Figure 3B. Mice were immunized with DEL conjugated SRBC on days 0 and 4 and their spleens analyzed 15 days following first DEL-SRBC immunization as shown in figure 3B. (**A**) Total GC cells ($B220^+Fas^+CD38^-$) per spleen from individual mice. (**B**) Total SW_{HEL} GC ($B220^+Fas^+CD38^-CD45.1^+CD45.2^-$) per spleen from individual mice. (**C**) Total SW_{HEL} GC per spleen that do not bind to HEL^{3X} at 0.14uM from individual mice. (**D**) Total SW_{HEL} GC per spleen bearing I29F mutations from individual mice. (**E**) The percentage of $CD45.1^+$ SW_{HEL} cells among total GC cells. (**F**) The percentage of $CD45.1^+$ SW_{HEL} cells bearing I29F mutations. (**G**) Ratio of SW_{HEL} GC cells that preferentially bind foreign (DEL) over self (HEL^{3X}) in individual mice. (**H**) Representative flow cytometric analysis of binding to self (0.14uM HEL^{3X}) and cell surface IgG1 or foreign (DEL) proteins, gated on $B220^+Fas^+CD38^-CD45.1^+CD45.2^-$ self-reactive or non self-reactive SW_{HEL} GC B-cells. Mean ± SEM displayed for each quandrant. (**I**) Summary of mutations at H-chain I29, S52, Y53, and Y58 in individually

sorted and sequenced SW_{HEL} cells. Colour coding denotes the consequence of each mutation for self-affinity. Each column represents a single cell, each row denotes whether that cell has a mutation at the indicated amino acid position, and all the cells from a single mouse are grouped within red or black boxes. (**J**) The percentage of SW_{HEL} cells with substitutions at each H-chain amino acid.

Data points represent one mouse. NS $P>0.05$, * $P<0.05$ ** $P<0.01$. Student's *t*-test. Data in A-F and H-J are pooled from at least two independent experiments, each involving 3-5 mice per group. Data in G represents one experiment.

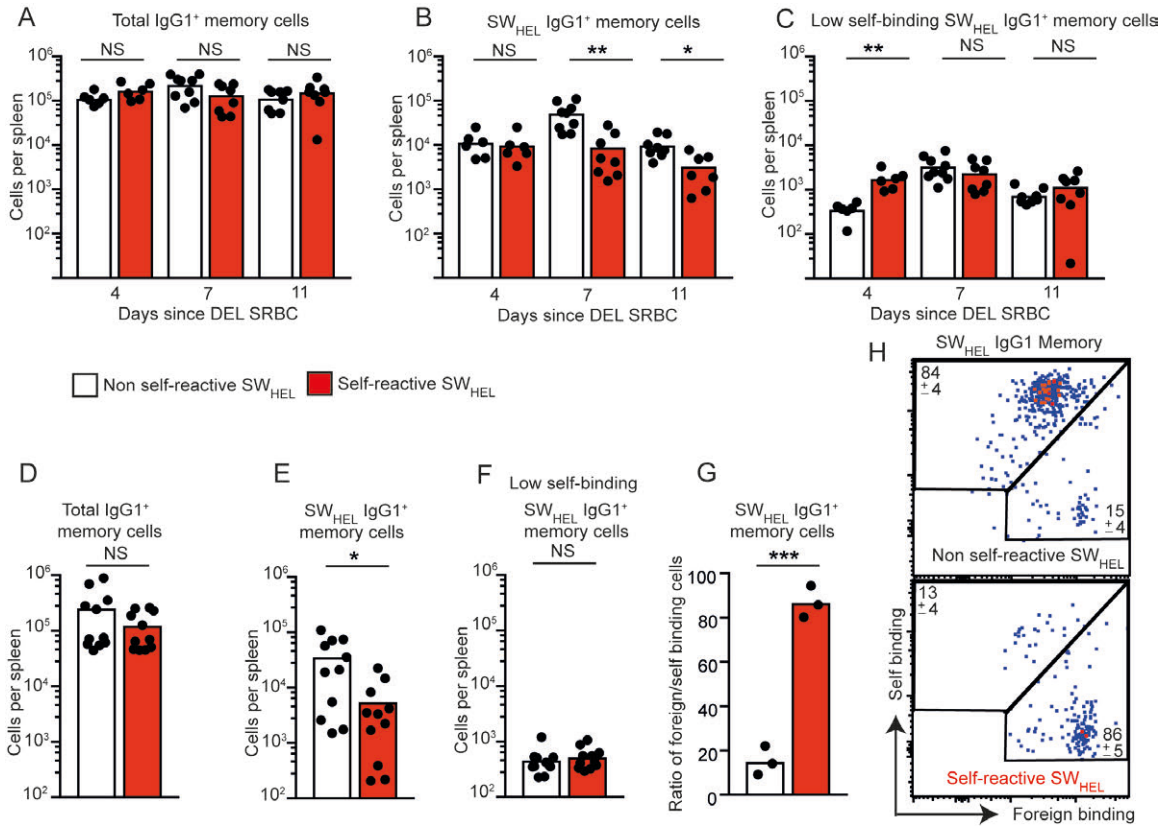

Fig. S10.

IgG1 SW_{HEL} memory response. (**A-C**) Mice were first immunized with unconjugated SRBC to initiate GC reactions and boosted with DEL-SRBC to activate SW_{HEL} cells and their spleens analyzed 4, 7 and 11 days following DEL-SRBC immunization as shown in figure 3A. (**A**) Total IgG1 switched memory cells ($B220^+Fas^-CD38^+IgG1^+$) per spleen from individual mice at the indicated timepoints. (**B**) Total SW_{HEL} IgG1 switched memory cells ($B220^+Fas^-CD38^+IgG1^+CD45.1^+CD45.2^-$) per spleen from individual mice at the indicated timepoints. (**C**) Total SW_{HEL} IgG1 switched memory cells per spleen that do not bind to HEL^{3X} at 0.14 μM from individual mice at the indicated timepoints.

(**D-H**) Mice were immunized with DEL-SRBC on days 0 and 4 and analyzed day 15 as shown in figure 3B. (**D**) Total IgG1 switched memory cells ($B220^+Fas^-CD38^+IgG1^+$) per spleen. (**E**) Total SW_{HEL} IgG1 switched memry cells ($B220^+Fas^-CD38^+IgG1^+CD45.1^+CD45.2^-$) per spleen from individual mice. (**F**) Total SW_{HEL} IgG1 switched memory cells per spleen that do not bind to HEL^{3X} at 0.14 μM from individual mice. (**G**) Ratio of SW_{HEL} IgG1 memory cells that preferentially bind foreign (DEL) over self (HEL^{3X}) in individual mice. (**H**) Representative flow cytometric analysis of relative binding of individual SW_{HEL} IgG1 memory cells to soluble monomeric self (HEL^{3X}) and foreign (DEL) proteins. Mean ± SEM displayed for each gate.

Data points represent one mouse. NS $P>0.05$, * $P<0.05$ ** $P<0.01$ *** $P<0.001$. Student's *t*-test. Data in A-F are pooled from at least two independent experiments, each involving 2-5 mice per group. Data in G and H represents one experiment.

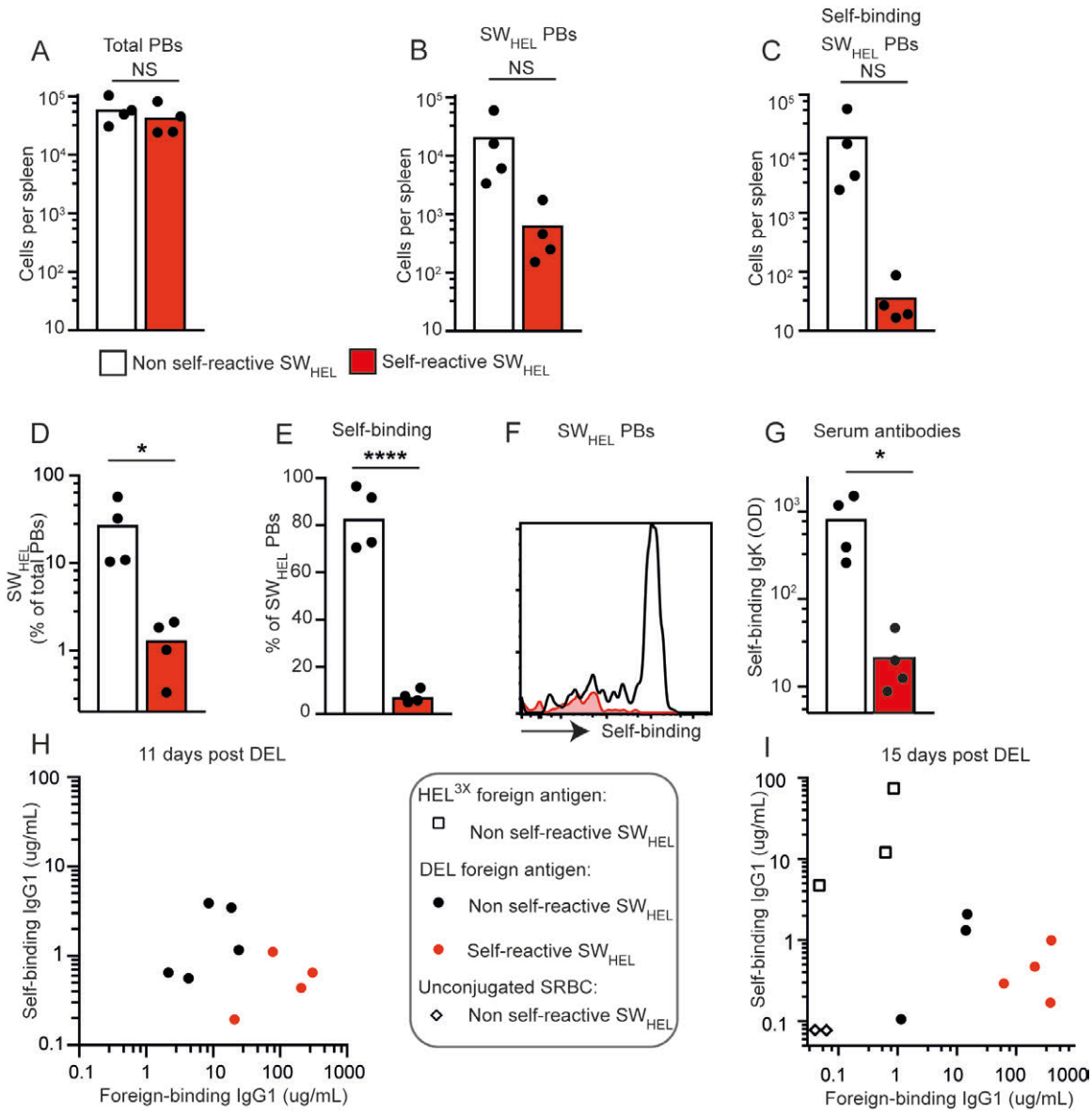

Fig. S11.

Early plasmablast (PB) and serum antibody response.

(**A-H**) Mice were first immunized with unconjugated SRBC to initiate GC reactions and boosted with DEL-SRBC to activate SW_{HEL} cells and their spleens analyzed 4 days following DEL-SRBC immunization as shown in figure 2A. (**A**) Total PBs ($B220^{+}Fas^{-}CD38^{-}IgD^{-}TACI^{+}CD138^{+}$) per spleen. (**B**) Total SW_{HEL} PBs ($B220^{+}Fas^{-}CD38^{-}IgD^{-}TACI^{+}CD138^{+}CD45.1^{+}CD45.2^{-}$) per spleen. (**C**) Total SW_{HEL} PBs per spleen that have retained binding to self (HEL^{3X}) at 0.14μM. (**D**) The percentage of $CD45.1^{+}$ SW_{HEL} PBs among total PBs. (**E**) The percentage of SW_{HEL} PBs that have retained binding to self. (**F**) Representative histograms of SW_{HEL} PBs showing self-binding. (**G**) Serum antibody ELISA showing self binding Igκ. (**H**) Serum antibody ELISA showing self and foreign (DEL) binding IgG1.

(**I**) Serum antibody ELISA showing self and foreign binding IgG1 from individual mice immunized with DEL-SRBC on days 0 and 4 and then harvested 15 days post DEL-

SRBC as shown in figure 3B.
Data points represent one mouse. NS P>0.05, * P<0.05 **** P<0.0001. Student's *t*-test.
Data are representative of one experiment, with 3-5 mice per group.

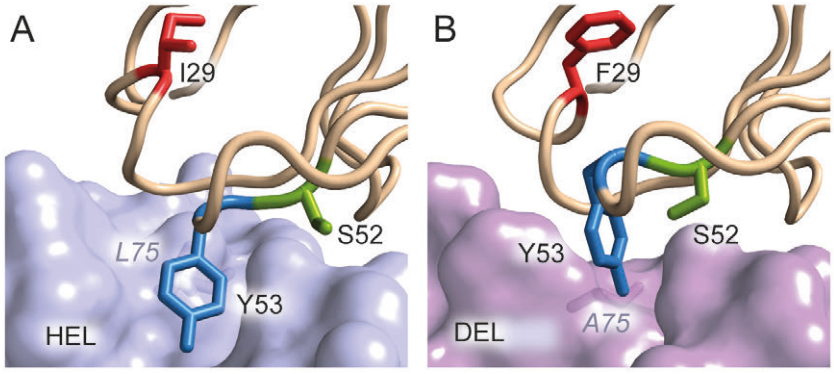

Fig. S12.
X-ray crystallographic structure of unmutated HyHEL10 in complex with HEL (**A**) and HyHEL10^{I29F} mutant antibody in complex with DEL (**B**).

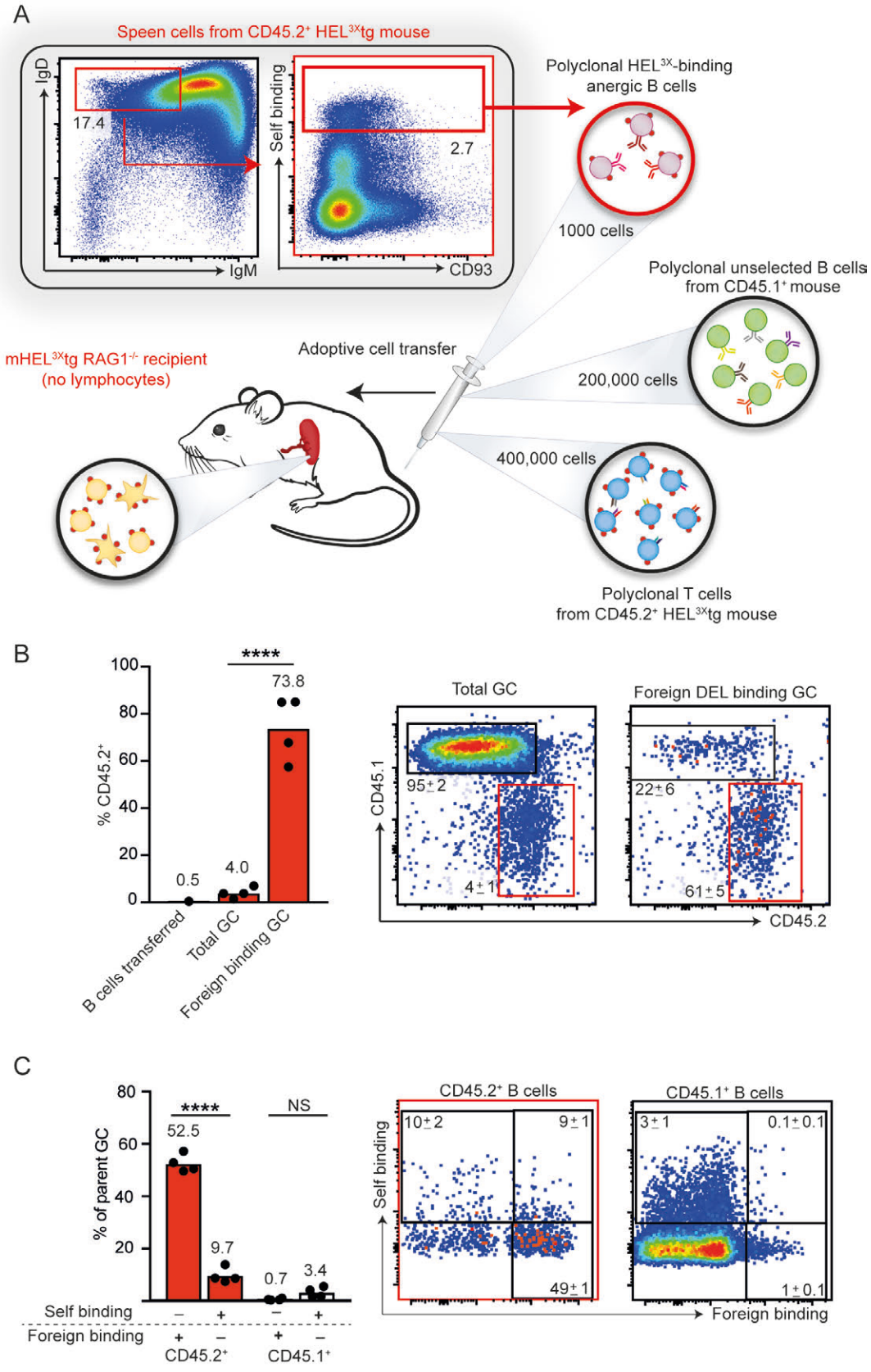
A
Speen cells from CD45.2+ HEL3Xtg mouse
IgD
17.4
IgM
Self binding
2.7
CD93
Polyclonal HEL3X-binding anergic B cells
1000 cells
Polyclonal unselected B cells from CD45.1+ mouse
200,000 cells
400,000 cells
Polyclonal T cells from CD45.2+ HEL3Xtg mouse
mHEL3Xtg RAG1-/- recipient (no lymphocytes)
Adoptive cell transfer
B
% CD45.2+
****
73.8
4.0
0.5
B cells transferred
Total GC
Foreign binding GC
Total GC
Foreign DEL binding GC
CD45.1
95±2
4±1
22±6
61±5
CD45.2
C
% of parent GC
****
NS
52.5
9.7
0.7
3.4
Self binding
Foreign binding
CD45.2+
CD45.1+
CD45.2+ B cells
CD45.1+ B cells
Self binding
10±2
9±1
49±1
3±1
0.1±0.1
1±0.1
Foreign binding

Fig. S13.

(Fig. S13 cont'd) Resolution of antigenic mimicry by rapid evolution of polyclonal self-reactive B-cells to lose self-binding and retain foreign specificity.
(**A**) Flow cytometric analysis of spleen B-cells pooled from mice with a normal antibody repertoire expressing HEL^{3X} as a ubiquitious membrane self antigen. B-cells with anergic IgD^{+} IgM^{low} phenotype were gated, and further subdivided to sort the subset staining brightly with 0.14 uM monomeric HEL^{3X}, comprising 0.5% of all B-cells. The percentage of parent cells within the indicated gates is shown. Sorted polyclonal HEL^{3X}-binding anergic B-cells ($CD45.2^{+}$) were mixed with unselected spleen B-cells ($CD45.1^{+}$) to comprise 0.5% of the mixture, and transferred by intravenous injection together with T-cells into $mHEL^{3X}$ tg *Rag1*$^{-/-}$ mice so that the transferred B-cells could be tracked by flow cytometry. The recipient mice were immunized with foreign DEL-SRBC on days 0 and 4, boosted with DEL conjugated to horse red blood cells (HRBCs) on day 14, and splenocytes analyzed by flow cytometry on day 20. (**B**) $CD45.2^{+}$ B-cells, derived from the sorted polyclonal HEL^{3X}-binding anergic B-cell inoculum, were enumerated by flow cytometry as a percentage of all B-cells, either in the transferred mixture (left), among all GC B-cells ($B220^{+}Fas^{+}CD38^{-}$) on day 20 (middle), and among the subset of GC B-cells binding to foreign DEL-biotin on day 20 (right). Representative flow cytometric plots from day 20 are shown. Numbers show mean percentage and s.e.m of cells in each gate. (**C**) GC cells on day 20 were stained first with 0.14μM monomeric HEL^{3X} and then with DEL-biotin, and analyzed by flow cytometry to enumerate the percentage of $CD45.2^{+}$ or $CD45.1^{+}$ GC cells that selectively bound the foreign or self lysozymes.
Data points represent one mouse. NS $P>0.05$ **** $P<0.0001$. Student's *t*-test. Data shown from one experiment, representative of two, with 4 mice per group.

HEL^{3X} affinities (SELF)								
Mutant	K_D	k_a	k_d	K_A	Affinity	Fold change	ΔΔG apparent (kcal/mol)	Expected additive ΔΔG (kcal/mol)
WT	$8.43x10^{-8}$	$1.49x10^{5}$	$1.26x10^{-2}$	$1.19x10^{7}$	84nM	0.0	0.0	
I29F	$8.81x10^{-7}$	$1.01x10^{5}$	$8.89x10^{-2}$	$1.14x10^{6}$	880nM	-10.5	1.4	
S52T	$1.67x10^{-7}$	$1.21x10^{5}$	$2.03x10^{-2}$	$5.98x10^{6}$	167nM	-2.0	0.4	
Y53F	$1.64x10^{-7}$	$1.21x10^{5}$	$1.98x10^{-2}$	$6.11x10^{6}$	164nM	-1.9	0.4	
Y58F	$3.28x10^{-8}$	$2.16x10^{5}$	$7.09x10^{-3}$	$3.05x10^{7}$	33nM	2.6	-0.6	
I29F/S52T	$6.10x10^{-7}$	$6.98x10^{4}$	$4.26x10^{-2}$	$1.64x10^{6}$	610nM	-7.2	1.2	1.8
I29F/Y53F	$7.98x10^{-7}$	$9.85x10^{4}$	$7.86x10^{-2}$	$1.25x10^{6}$	798nM	-9.5	1.3	1.8
S52T/Y58F	$5.14x10^{-8}$	$1.89x10^{5}$	$9.69x10^{-3}$	$1.95x10^{7}$	51nM	1.6	-0.3	-0.2
I29F/S52T/Y58F	$1.13x10^{-7}$	$1.14x10^{5}$	$1.28x10^{-2}$	$8.88x10^{6}$	113nM	-1.3	0.2	1.2
S52T/Y53F	$1.52x10^{-7}$	$1.12x10^{5}$	$1.71x10^{-2}$	$6.58x10^{6}$	152nM	-1.8	0.3	0.8
S52T/Y53F/Y58F	$2.44x10^{-8}$	$2.08x10^{5}$	$5.07x10^{-3}$	$4.11x10^{7}$	24nM	3.5	-0.7	0.2
I29F/S52T/Y53F	$8.07x10^{-7}$	$8.64x10^{4}$	$6.97x10^{-2}$	$1.24x10^{6}$	807nM	-9.6	1.3	2.2
S52R	Does not bind at 5uM				N/A	N/A		
S52R/Y53F	Does not bind at 5uM				N/A	N/A		

DEL affinities (FOREIGN)								
Mutant	K_D	k_a	k_d	K_A	Affinity	Fold change	ΔΔG apparent (kcal/mol)	Expected additive ΔΔG (kcal/mol)
WT	$4.01x10^{-8}$	$1.85x10^{5}$	$7.40x10^{-3}$	$2.49x10^{7}$	40nM	0.0	0.0	
I29F	$1.57x10^{-8}$	$1.76x10^{5}$	$2.76x10^{-3}$	$6.37x10^{7}$	15nM	2.6	-0.6	
S52T	$3.35x10^{-8}$	$1.73x10^{5}$	$5.79x10^{-3}$	$2.98x10^{7}$	33nM	1.2	-0.1	
Y53F	$8.35x10^{-9}$	$2.18x10^{5}$	$1.82x10^{-3}$	$1.20x10^{8}$	8nM	4.8	-0.9	
Y58F	$1.07x10^{-8}$	$2.63x10^{5}$	$2.81x10^{-3}$	$9.35x10^{7}$	11nM	3.8	-0.8	
I29F/S52T	$5.79x10^{-9}$	$1.55x10^{5}$	$8.97x10^{-4}$	$1.73x10^{8}$	6nM	6.9	-1.1	-0.7
I29F/Y53F	$1.03x10^{-9}$	$1.47x10^{5}$	$1.52x10^{-4}$	$9.70x10^{8}$	1nM	39.0	-2.2	-1.5
S52T/Y58F	$2.62x10^{-9}$	$1.74x10^{5}$	$4.58x10^{-4}$	$3.80x10^{8}$	3nM	15.3	-1.6	-0.9
I29F/S52T/Y58F	$1.69x10^{-9}$	$1.91x10^{5}$	$3.22x10^{-4}$	$5.92x10^{8}$	2nM	23.8	-1.9	-1.5
S52T/Y53F	$3.56x10^{-9}$	$2.00x10^{5}$	$7.11x10^{-4}$	$2.81x10^{8}$	3.6nM	11.1	-1.4	-1.0
S52T/Y53F/Y58F	$5.02x10^{-10}$	$2.54x10^{5}$	$1.27x10^{-4}$	$1.99x10^{9}$	500pM	80.0	-2.6	-1.6
I29F/S52T/Y53F	$1.64x10^{-10}$	$3.18x10^{5}$	$5.22x10^{-5}$	$6.10x10^{9}$	164pM	245.0	-3.3	-1.6
S52R	Does not bind at 5uM				N/A	N/A		
S52R/Y53F	Does not bind at 5uM				N/A	N/A		

I29F single mutant binding to:	K_D	k_a	k_d	K_A	Affinity	Fold change
DEL (foreign)	$1.57x10^{-8}$	$1.76x10^{5}$	$2.76x10^{-3}$	$6.37x10^{7}$	15nM	0.0
HEL R21Q R73E D101R (self)	$8.81x10^{-7}$	$1.01x10^{5}$	$8.89x10^{-2}$	$1.14x10^{6}$	880nM	-56.1
HEL R21Q R73E L75A D101R (self with foreign 75)	$8.56x10^{-7}$	$9.34x10^{4}$	$7.99x10^{-2}$	$1.17x10^{6}$	856nM	-54.5
HEL R21Q R73K D101R (self with foreign 73)	$3.50x10^{-7}$	$1.92x10^{5}$	$6.73x10^{-2}$	$2.86x10^{6}$	350nM	-22.3
HEL R21Q R73K L75A D101R (self with foreign 73, 75)	$2.77x10^{-8}$	$3.61x10^{5}$	$1.00x10^{-2}$	$3.61x10^{7}$	28nM	-1.8
HEL R21Q G71R R73K L75A N77G D101R (self with foreign 71, 73, 75, 77)	$3.18x10^{-8}$	$3.51x10^{5}$	$1.12x10^{-2}$	$3.14x10^{7}$	32nM	-2.0

Table S1.

(Table S1 cont'd)
Binding kinetics of interactions between soluble monomeric self (HEL^{3X}) or foreign (DEL) and immobilised HyHEL10 antibody mutant FAbs, as measured by bio-layer interferometry. Also tested was binding of self-proteins with the indicated residues substituted from the self to the foreign sequence. Soluble antigen was run over immobilized HyHEL10 variants at four different concentrations to obtain global fits of binding kinetics for each interaction using the BLItz Pro 1.2 software (ForteBio). The utilized concentrations of antigen differed for each HyHEL10 variant, but all fell within a range from 5 nM (lowest foreign molarity used for $HyHEL10^{I29F/S52T/Y53F}$) to 5 μM (highest self molarity used for $HyHEL10^{I29F}$, $HyHEL10^{I29F/Y53F}$ and $HyHEL10^{I29F/S52T/Y53F}$). Equilibrium dissociation constants (K_D, M), association constants (k_a, $M^{-1}s^{-1}$), dissociation rate constants (k_d, s^{-1}) and affinity binding constants (K_A, M^{-1}), are shown for each interaction as well as the fold change in affinity compared to unmutated HyHEL10. Differential binding energies (ΔΔG) are calculated according to (*31*) and the apparent values are shown for each individual, pair or trio of mutations. For comparison an additional column provides the expected ΔΔG for each pair or trio of mutations based on additive effects of the individual mutations, highlighting epistatic interactions.

Data collection statistics		
Crystal	**HyHEL10-I29F:DEL-I**	**HyHEL10-I29F-S52T-Y53F:DEL-I**
Wavelength	0.9537	0.9537
Spacegroup	P 2_1 2 2_1	P 2_1 2_1 2_1
Unit cell dimensions: a, b, c (Å); α, β, γ, (°)	89.02, 102.91, 133.98; *90.0, 90.0, 90.0*	88.65, 132.66, 199.11; *90.0, 90.0, 90.0*
Resolution range	2.43-47.49 (2.43-2.51)	1.90-49.78 (1.90-1.93)
Total reflections	459,563 (43,523)	1,484,865 (69,377)
Unique reflections	47,296 (4,593)	180,881 (8,562)
Completeness	99.9 (100)	98.0 (94.6)
Multiplicity	9.7 (9.5)	8.2 (8.1)
Average (I/σ(I))	15.5 (3.3)	12.6 (2.8)
Mean half set correlation, $CC_{1/2}$	0.998 (0.850)	0.998 (0.642)
Rmeas (all I+ and I-)	0.100 (0.894)	0.105 (0.838)
Rpim (all I+ and I-)	0.032 (0.261)	0.035 (0.286)
Wilson B (Å^2)	46.1	23.5
Refinement and model statistics		
Reflections used	44,719 (3,245)	171,765 (12,115)
R_{work}/R_{free}	0.262/0.296	0.193/0.235
Fab-DEL complexes/asu	2	4
Atoms protein	8176	16869
B average protein (Å^2)	61.9	29.5
Atoms non-protein	50	1034
B average non-protein (Å^2)	41.7	30.6
RMSD bond lengths (Å)	0.0108	0.0119
RMSD bond angles (°)	1.44	1.54
Ramachandran Outliers (%)	0.37	0.05
Ramachandran Favored (%)	97.2	98.1
PDB entry	**5VJO**	**5VJQ**

$$R_{meas} = \frac{\sum_{hkl}\sqrt{\frac{n}{n-1}}\sum_{i=1}^{n}|I_i(hkl) - \bar{I}(hkl)|}{\sum_{hkl}\sum_{i=1}^{n} I_i(hkl)} \quad R_{pim}$$

$$= \frac{\sum_{hkl}\sqrt{\frac{1}{n-1}}\sum_{i=1}^{n}|I_i(hkl) - \bar{I}(hkl)|}{\sum_{hkl}\sum_{i=1}^{n} I_i(hkl)}$$

$$R_{work}, R_{free} = \frac{\sum_{hkl}|F_{obs}(hkl) - F_{calc}(hkl)|}{\sum_{hkl} F_{obs}(hkl)}$$

$CC_{1/2}$ = Correlation coefficient between the averages of two randomly binned subsets of measurements for each reflection.

Table S2.
Diffraction data, structure refinement and model statistics. Values in parentheses contain data for the highest resolution shell. Diffraction data statistics ouput by AIMLESS (*30*). Ramachandran statistics output by MOLPROBITY (*35*).

Movie S1

Comparison of the structure of unmutated HyHEL10 in complex with HEL versus HyHEL10^{I29F,S52T,Y53F} triple mutant antibody in complex with DEL.

References and Notes

1. B. R. Wakerley, N. Yuki, Infectious and noninfectious triggers in Guillain-Barré syndrome. *Expert Rev. Clin. Immunol.* **9**, 627–639 (2013). doi:10.1586/1744666X.2013.811119 Medline

2. B. F. Haynes, J. Fleming, E. W. St. Clair, H. Katinger, G. Stiegler, R. Kunert, J. Robinson, R. M. Scearce, K. Plonk, H. F. Staats, T. L. Ortel, H. X. Liao, S. M. Alam, Cardiolipin polyspecific autoreactivity in two broadly neutralizing HIV-1 antibodies. *Science* **308**, 1906–1908 (2005). doi:10.1126/science.1111781 Medline

3. D. D. Pinschewer, M. Perez, E. Jeetendra, T. Bächi, E. Horvath, H. Hengartner, M. A. Whitt, J. C. de la Torre, R. M. Zinkernagel, Kinetics of protective antibodies are determined by the viral surface antigen. *J. Clin. Invest.* **114**, 988–993 (2004). doi:10.1172/JCI200422374 Medline

4. R. Wyatt, P. D. Kwong, E. Desjardins, R. W. Sweet, J. Robinson, W. A. Hendrickson, J. G. Sodroski, The antigenic structure of the HIV gp120 envelope glycoprotein. *Nature* **393**, 705–711 (1998). doi:10.1038/31514 Medline

5. H. B. Gristick, L. von Boehmer, A. P. West Jr., M. Schamber, A. Gazumyan, J. Golijanin, M. S. Seaman, G. Fätkenheuer, F. Klein, M. C. Nussenzweig, P. J. Bjorkman, Natively glycosylated HIV-1 Env structure reveals new mode for antibody recognition of the CD4-binding site. *Nat. Struct. Mol. Biol.* **23**, 906–915 (2016). doi:10.1038/nsmb.3291 Medline

6. D. Nemazee, M. Weigert, Revising B cell receptors. *J. Exp. Med.* **191**, 1813–1817 (2000). doi:10.1084/jem.191.11.1813 Medline

7. J. Tan, K. Pieper, L. Piccoli, A. Abdi, M. F. Perez, R. Geiger, C. M. Tully, D. Jarrossay, F. Maina Ndungu, J. Wambua, P. Bejon, C. S. Fregni, B. Fernandez-Rodriguez, S. Barbieri, S. Bianchi, K. Marsh, V. Thathy, D. Corti, F. Sallusto, P. Bull, A. Lanzavecchia, A LAIR1 insertion generates broadly reactive antibodies against malaria variant antigens. *Nature* **529**, 105–109 (2016). doi:10.1038/nature16450 Medline

8. J. H. Reed, J. Jackson, D. Christ, C. C. Goodnow, Clonal redemption of autoantibodies by somatic hypermutation away from self-reactivity during human immunization. *J. Exp. Med.* **213**, 1255–1265 (2016). doi:10.1084/jem.20151978 Medline

9. Z. Sabouri, P. Schofield, K. Horikawa, E. Spierings, D. Kipling, K. L. Randall, D. Langley, B. Roome, R. Vazquez-Lombardi, R. Rouet, J. Hermes, T. D. Chan, R. Brink, D. K. Dunn-Walters, D. Christ, C. C. Goodnow, Redemption of autoantibodies on anergic B cells by variable-region glycosylation and mutation away from self-reactivity. *Proc. Natl. Acad. Sci. U.S.A.* **111**, E2567–E2575 (2014). doi:10.1073/pnas.1406974111

10. T. G. Phan, M. Amesbury, S. Gardam, J. Crosbie, J. Hasbold, P. D. Hodgkin, A. Basten, R. Brink, B cell receptor-independent stimuli trigger immunoglobulin (Ig) class switch recombination and production of IgG autoantibodies by anergic self-reactive B cells. *J. Exp. Med.* **197**, 845–860 (2003). doi:10.1084/jem.20022144 Medline

11. T. G. Phan, D. Paus, T. D. Chan, M. L. Turner, S. L. Nutt, A. Basten, R. Brink, High affinity germinal center B cells are actively selected into the plasma cell compartment. *J. Exp. Med.* **203**, 2419–2424 (2006). doi:10.1084/jem.20061254 Medline

12. E. A. Padlan, E. W. Silverton, S. Sheriff, G. H. Cohen, S. J. Smith-Gill, D. R. Davies, Structure of an antibody-antigen complex: Crystal structure of the HyHEL-10 Fab-

lysozyme complex. *Proc. Natl. Acad. Sci. U.S.A.* **86**, 5938–5942 (1989). doi:10.1073/pnas.86.15.5938 Medline

13. D. Paus, T. G. Phan, T. D. Chan, S. Gardam, A. Basten, R. Brink, Antigen recognition strength regulates the choice between extrafollicular plasma cell and germinal center B cell differentiation. *J. Exp. Med.* **203**, 1081–1091 (2006). doi:10.1084/jem.20060087 Medline

14. T. D. Chan, K. Wood, J. R. Hermes, D. Butt, C. J. Jolly, A. Basten, R. Brink, Elimination of germinal-center-derived self-reactive B cells is governed by the location and concentration of self-antigen. *Immunity* **37**, 893–904 (2012). doi:10.1016/j.immuni.2012.07.017 Medline

15. J. G. Cyster, S. B. Hartley, C. C. Goodnow, Competition for follicular niches excludes self-reactive cells from the recirculating B-cell repertoire. *Nature* **371**, 389–395 (1994). doi:10.1038/371389a0 Medline

16. D. A. Fulcher, A. Basten, Reduced life span of anergic self-reactive B cells in a double-transgenic model. *J. Exp. Med.* **179**, 125–134 (1994). doi:10.1084/jem.179.1.125 Medline

17. C. C. Goodnow, J. Crosbie, S. Adelstein, T. B. Lavoie, S. J. Smith-Gill, R. A. Brink, H. Pritchard-Briscoe, J. S. Wotherspoon, R. H. Loblay, K. Raphael, R. J. Trent, A. Basten, Altered immunoglobulin expression and functional silencing of self-reactive B lymphocytes in transgenic mice. *Nature* **334**, 676–682 (1988). doi:10.1038/334676a0 Medline

18. M. P. Cooke, A. W. Heath, K. M. Shokat, Y. Zeng, F. D. Finkelman, P. S. Linsley, M. Howard, C. C. Goodnow, Immunoglobulin signal transduction guides the specificity of B cell-T cell interactions and is blocked in tolerant self-reactive B cells. *J. Exp. Med.* **179**, 425–438 (1994). doi:10.1084/jem.179.2.425 Medline

19. M. Acchione, C. A. Lipschultz, M. E. DeSantis, A. Shanmuganathan, M. Li, A. Wlodawer, S. Tarasov, S. J. Smith-Gill, Light chain somatic mutations change thermodynamics of binding and water coordination in the HyHEL-10 family of antibodies. *Mol. Immunol.* **47**, 457–464 (2009). doi:10.1016/j.molimm.2009.08.018 Medline

20. F. M. Burnet, *The Clonal Selection Theory of Acquired Immunity* (Vanderbilt Univ. Press, 1959).

21. J. Lederberg, Genes and antibodies. *Science* **129**, 1649–1653 (1959). doi:10.1126/science.129.3364.1649 Medline

22. H. Wardemann, S. Yurasov, A. Schaefer, J. W. Young, E. Meffre, M. C. Nussenzweig, Predominant autoantibody production by early human B cell precursors. *Science* **301**, 1374–1377 (2003). doi:10.1126/science.1086907 Medline

23. N. K. Jerne, The somatic generation of immune recognition. *Eur. J. Immunol.* **1**, 1–9 (1971). doi:10.1002/eji.1830010102 Medline

24. D. Nemazee, Antigen receptor ‘capacity’ and the sensitivity of self-tolerance. *Immunol. Today* **17**, 25–29 (1996). doi:10.1016/0167-5699(96)80565-2 Medline

25. A. S. Perelson, G. F. Oster, Theoretical studies of clonal selection: Minimal antibody repertoire size and reliability of self-non-self discrimination. *J. Theor. Biol.* **81**, 645–670 (1979). doi:10.1016/0022-5193(79)90275-3 Medline

26. P. Mombaerts, J. Iacomini, R. S. Johnson, K. Herrup, S. Tonegawa, V. E. Papaioannou, RAG-1-deficient mice have no mature B and T lymphocytes. *Cell* **68**, 869–877 (1992). doi:10.1016/0092-8674(92)90030-G Medline

27. D. B. Langley, B. Crossett, P. Schofield, J. Jackson, M. Zeraati, D. Maltby, M. Christie, D. Burnett, R. Brink, C. Goodnow, D. Christ, Structural basis of antigen recognition: Crystal structure of duck egg lysozyme. *Acta Crystallogr. D* **73**, 910–920 (2017). doi:10.1107/S2059798317013730 Medline

28. R. Vazquez-Lombardi, D. Nevoltris, A. Luthra, P. Schofield, C. Zimmermann, D. Christ, Transient expression of human antibodies in mammalian cells. *Nat. Protoc.* **13**, 99–117 (2018). doi:10.1038/nprot.2017.126 Medline

29. T. G. G. Battye, L. Kontogiannis, O. Johnson, H. R. Powell, A. G. W. Leslie, *iMOSFLM*: A new graphical interface for diffraction-image processing with *MOSFLM*. *Acta Crystallogr. D* **67**, 271–281 (2011). doi:10.1107/S0907444910048675 Medline

30. P. R. Evans, An introduction to data reduction: Space-group determination, scaling and intensity statistics. *Acta Crystallogr. D* **67**, 282–292 (2011). doi:10.1107/S090744491003982X Medline

31. G. Schreiber, A. R. Fersht, Energetics of protein-protein interactions: Analysis of the barnase-barstar interface by single mutations and double mutant cycles. *J. Mol. Biol.* **248**, 478–486 (1995). Medline

32. A. J. McCoy, R. W. Grosse-Kunstleve, P. D. Adams, M. D. Winn, L. C. Storoni, R. J. Read, *Phaser* crystallographic software. *J. Appl. Crystallogr.* **40**, 658–674 (2007). doi:10.1107/S0021889807021206 Medline

33. G. N. Murshudov, P. Skubák, A. A. Lebedev, N. S. Pannu, R. A. Steiner, R. A. Nicholls, M. D. Winn, F. Long, A. A. Vagin, *REFMAC*5 for the refinement of macromolecular crystal structures. *Acta Crystallogr. D* **67**, 355–367 (2011). doi:10.1107/S0907444911001314 Medline

34. P. Emsley, B. Lohkamp, W. G. Scott, K. Cowtan, Features and development of *Coot*. *Acta Crystallogr. D* **66**, 486–501 (2010). doi:10.1107/S0907444910007493 Medline

35. V. B. Chen, W. B. Arendall 3rd, J. J. Headd, D. A. Keedy, R. M. Immormino, G. J. Kapral, L. W. Murray, J. S. Richardson, D. C. Richardson, *MolProbity*: All-atom structure validation for macromolecular crystallography. *Acta Crystallogr. D* **66**, 12–21 (2010). doi:10.1107/S0907444909042073 Medline